

# Collective excitations in spin-polarized bilayer graphene

Nguyen Van Men<sup>1,2</sup>, Nguyen Quoc Khanh<sup>3,4\*</sup>, and Dong Thi Kim Phuong<sup>5,4</sup>

<sup>1</sup>*Atomic Molecular and Optical Physics Research Group, Advanced Institute of Materials Science, Ton Duc Thang University, Ho Chi Minh City, Viet Nam (Email: [nguyenvanmen@tdtu.edu.vn](mailto:nguyenvanmen@tdtu.edu.vn))*

<sup>2</sup>*Faculty of Applied Sciences, Ton Duc Thang University, Ho Chi Minh City, Viet Nam.*

<sup>3</sup>*University of Science - VNUHCM, 227-Nguyen Van Cu Street, 5th District, Ho Chi Minh City, Viet Nam (Email: [nqkhanh@hcmus.edu.vn](mailto:nqkhanh@hcmus.edu.vn)).*

<sup>4</sup>*Vietnam National University, Ho Chi Minh City, Viet Nam.*

<sup>5</sup>*University of An Giang - VNUHCM, 18-Ung Van Khiem Street, Long Xuyen, An Giang, Viet Nam (Email: [dtkphuong@agu.edu.vn](mailto:dtkphuong@agu.edu.vn)).*

## Abstract

We calculate the plasmon frequency  $\omega$  and damping rate  $\gamma$  of plasma oscillations in a spin-polarized BLG system. Using the long wavelength approximation for dynamical dielectric function, we obtain an analytical expression for plasmon frequency showing that the degree of spin polarization  $P$  has negligible effect on the long wavelength plasmon frequency. Numerical calculations demonstrate that the degree of spin polarization affects slightly (strongly) plasmon frequency at small (large) wave-vectors and the maximum value of damping rate increases with increasing  $P$ . We also study the effects of carrier density and substrate dielectric constant on plasmon properties for different value of spin polarization. The numerically calculated critical wave-vector, at which the plasmon dispersion curve hits the edge of electron-hole continuum, decreases with  $P$  and can be used to determine experimentally the degree of spin polarization.

## 1. Introduction

Collective excitations in materials have lots of technological applications covering fields ranging from energy storage to optical and membrane technology. In the last decades, plasmon in ordinary two-dimensional electron gas (2DEG) systems has been studied intensively. Graphene, a perfect two-dimensional system, is considered as an excellent candidate replacing silicon materials used in recent years because of its unique electrical and optical properties [1-18]. It was shown that low-energy quasi-particles in bilayer graphene (BLG) behave as massive chiral fermions, compared to massive non-chiral (massless chiral) fermions in 2DEG (monolayer graphene (MLG)). Therefore, the density-density response function and dynamical dielectric function of BLG also differ significantly from those of 2DEG and MLG. As a result, screening effects and collective excitations in BLG show also different features [19-26].

In the presence of in-plane external magnetic field, carriers in graphene systems are spin polarized with negligible magneto-orbital coupling effect due to one-atom thickness of graphene. Previous researches have discovered that the spin polarization can change substantially the characters of 2DEG systems [27-31]. Recently, the authors of Ref. [32] have found remarkable differences in plasmon properties of spin-polarized MLG, compared to those of unpolarized one. It is known that plasmons in BLG differs pronouncedly from those in MLG. Hence, collective excitations in spin-polarized BLG may demonstrate some new interesting features different from those of spin-polarized MLG. Up to now, however, no calculations on the collective excitations in spin-polarized BLG has been carried out. Therefore, in this paper, using random-phase-approximation (RPA), we investigate plasmon properties of a spin-polarized BLG system.

## 2. Theory

We consider a zero-temperature, spin-polarized BLG system with a low energy parabolic dispersion relation. The polarization is assumed to be induced by an in-plane Zeeman field  $\vec{B}$ . Under the magnetic field  $B$ , the energy of electrons in BLG at a given wave vector  $\vec{k}$  can be written as [19-20, 32]:

$$E_{\vec{k}}^{\lambda,\sigma} = \lambda \frac{\hbar^2 k^2}{2m^*} + \sigma g^* \mu_B B \quad (1)$$

---

\* Corresponding author: [nqkhanh@hcmus.edu.vn](mailto:nqkhanh@hcmus.edu.vn) (N.Q. Khanh).

where,  $\lambda = \pm 1$  denotes electrons in conduction and valence band,  $\mu_B$  is the Bohr magneton,  $\sigma = \pm 1$  indicates spin-up and spin-down electrons,  $g^*$  is the electron Landé  $g$ -factor and  $m^* = 0.033m_0$ , with  $m_0$  being the free electron mass, is the effective mass of electrons in BLG.

Collective excitations in the system can be obtained from the zeroes of dynamical dielectric function [32-43]

$$\varepsilon(q, \omega - i\gamma) = 0 \quad (2)$$

In case of weak damping ( $\gamma \ll \omega$ ), the plasmon dispersion and decay rate are determined from the following equations [32-43]

$$\text{Re} \varepsilon(q, \omega_p) = 0 \quad (3)$$

and

$$\gamma = \text{Im} \varepsilon(q, \omega_p) \left( \left. \frac{\partial \text{Re} \varepsilon(q, \omega)}{\partial \omega} \right|_{\omega=\omega_p} \right)^{-1} \quad (4)$$

Within RPA, the dynamical dielectric function of spin-polarized BLG has the form [32-43]

$$\varepsilon(q, \omega) = 1 - v(q) \Pi(q, \omega) \quad (5)$$

where  $v(q) = 2\pi e^2 / (\kappa q)$ , with  $\kappa$  being the background static dielectric constant, denotes the bare Coulomb interaction of electrons in momentum space and  $\Pi(q, \omega)$  is the response function of spin-polarized BLG [19-21, 32]

$$\Pi(q, \omega) = \Pi_{\uparrow}^0(q, \omega) + \Pi_{\downarrow}^0(q, \omega) \quad (6)$$

with

$$\Pi_{\sigma}^0(q, \omega) = g_v \sum_{\lambda, \lambda', k} |g_k^{\lambda, \lambda'}(q)|^2 \left[ \frac{f(E_k^{\lambda, \sigma}) - f(E_{k+\bar{q}}^{\lambda', \sigma})}{\omega + E_k^{\lambda, \sigma} - E_{k+\bar{q}}^{\lambda', \sigma} + i\delta} \right] \quad (7)$$

In Eq. (7),  $g_v = 2$  indicates the valley degeneracy,  $f(x)$  is the Fermi – Dirac function, and

$$|g_k^{\lambda, \lambda'}(q)|^2 = \frac{1}{2} \left[ 1 + \lambda \lambda' \cos(2\theta_k - 2\theta_{k+\bar{q}}) \right] \quad (8)$$

is the overlap function.

In long wavelength limit ( $q \rightarrow 0$ ), the spin-resolved response function of spin-polarized BLG has simple form [19-21]

$$\Pi_{\sigma}^0(y, z) = \frac{g_v E_F}{2\pi} \left( \frac{y}{z} \right)^2 (1 + \sigma P) \quad (9)$$

where  $y = q / k_F$ ,  $z = \omega / E_F$ . Here  $E_F = \hbar^2 k_F^2 / (2m^*)$  and  $k_F = \sqrt{\pi n}$  are Fermi energy and Fermi wave-vector of unpolarized BLG with carrier density  $n = n_{\uparrow} + n_{\downarrow}$ , and  $P = (n_{\uparrow} - n_{\downarrow}) / (n_{\uparrow} + n_{\downarrow})$ , with  $n_{\sigma}$  being the spin-polarized electron density, denotes the degree of spin polarization. In this approximation, the solution of Eq. (3) can be easily obtained,

$$\omega^2 = \frac{2e^2 g_v E_F}{\kappa} q. \quad (10)$$

Eq. (10) shows that the plasmon frequency in spin-polarized BLG is almost independent of spin polarization in long wavelength limit. It is well-known that the plasmon mode is undamped until the dispersion curve hits the edge of single-particle-excitation (SPE) continuum, determined by equations  $\omega_1 = q^2 + 2q\sqrt{1 + \sigma P}$  and  $\omega_2 = q^2 - 2q\sqrt{1 + \sigma P} + 2(1 + \sigma P)$ , at a critical wave-vector  $q_c$ . In case of spin-polarized BLG  $q_c$  is determined by the intersection of plasmon dispersion curve with the lower edge of the inter-band continuum of minority spin carriers. In the limit  $q \rightarrow 0$ , using Eq. (10) we have

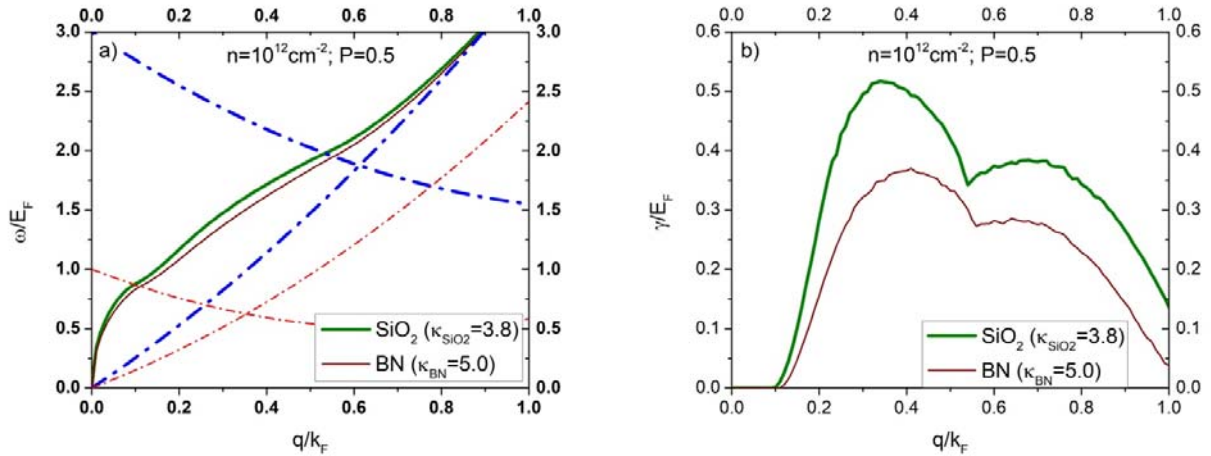
$$\frac{q_c}{k_F} = p + \frac{1}{2} \sqrt{-\frac{4p^2}{3} + \frac{4\sqrt[3]{2}(-3a_0^2 p + 4p^4)}{3\Delta(a_0, p)} + \frac{\Delta(a_0, p)}{3\sqrt[3]{2}}} + \frac{1}{2} \sqrt{\frac{8p^2}{3} - \frac{4\sqrt[3]{2}(-3a_0^2 p + 4p^4)}{3\Delta(a_0, p)} - \frac{\Delta(a_0, p)}{3\sqrt[3]{2}}} + \frac{2a_0^2}{\sqrt{-\frac{4p^2}{3} + \frac{4\sqrt[3]{2}(-3a_0^2 p + 4p^4)}{3\Delta(a_0, p)} + \frac{\Delta(a_0, p)}{3\sqrt[3]{2}}}} \quad (11)$$

where  $p = \sqrt{1 - P}$ ,  $a_0 = (2e/\hbar)\sqrt{g_v m^* / (\kappa k_F)}$  and  $\Delta(a_0, p) = [27a_0^4 + 144a_0^2 p^3 + 3a_0^2 \sqrt{3(27a_0^4 + 544a_0^2 p^3 - 512p^6)} - 128p^6]^{1/3}$ .

### 3. Results and discussions

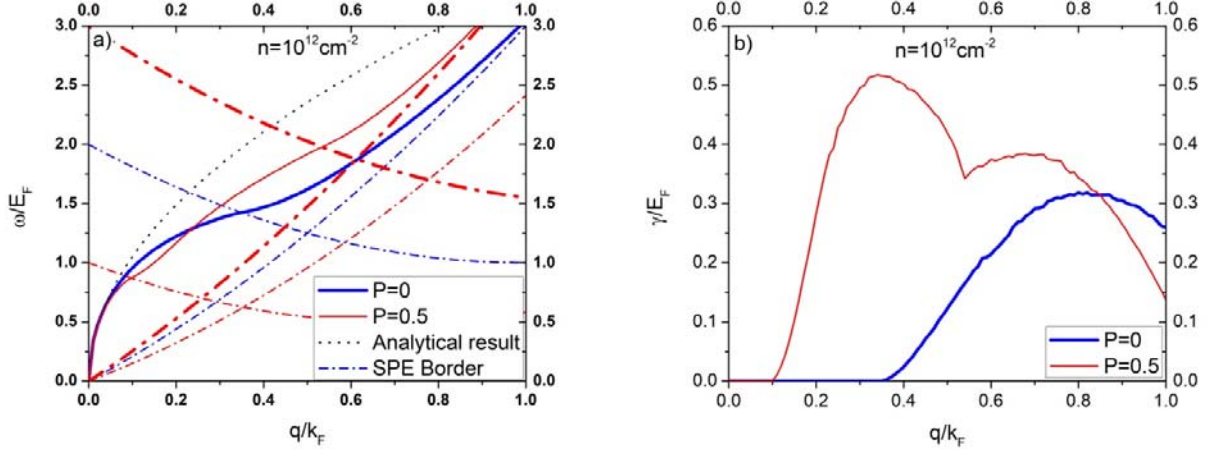
In this section, we present our numerical results for plasmon frequency and damping rate of spin-polarized BLG with spin polarization  $P$  and total carrier density  $n$ .

Figure 1 illustrates plasmon frequency (a) and damping rate (b) in a BLG system with  $n = 10^{12} \text{ cm}^{-2}$  and  $P = 0.5$  for two different substrates  $\text{SiO}_2$  ( $\kappa_{\text{SiO}_2} = 3.8$ ) [25] and BN (boron nitride,  $\kappa_{\text{BN}} = 5.0$ ) [44]. We observe that plasmon mode is undamped until the dispersion curve hits the edge of the single-particle-excitation (SPE) of minority spin carriers at  $q \approx 0.1k_F$ . In the SPE inter-band continuum of minority spin carriers the damping rate increases, reaches a peak and then decreases before the dispersion curve enters the SPE inter-band continuum of majority spin carriers at  $q \approx 0.54k_F$ . At larger wave-vectors damping rate increases again before decreasing to zero as plasmon approaches the intra-band continuum and vanishes. The increase in dielectric constant of substrate decreases significantly the plasmon frequency and damping rate as in unpolarized BLG [20].



**Fig. 1.** Plasmon frequency (a) and damping rate (b) in spin-polarized BLG with  $n = 10^{12} \text{ cm}^{-2}$ ,  $P = 0.5$  for two different substrates  $\text{SiO}_2$  ( $\kappa_{\text{SiO}_2} = 3.8$ ) and  $\text{BN}$  ( $\kappa_{\text{BN}} = 5.0$ ). Dashed-dotted lines show the boundaries of SPE continuum.

In order to see the effects of spin polarization on plasmon modes in spin-polarized BLG, we plot in Fig. 2 plasmon frequency (a) and damping rate (b) as a function of wave-vector for  $n=10^{12} \text{ cm}^{-2}$  in two cases  $P=0$  and  $P=0.5$ . The dotted line corresponds to analytical results given in Eq. (10) with the same system parameters. As seen from Fig. 2(a), the analytical results have a good agreement with the numerical ones in long wavelength region. Numerical results also indicate that in long wavelength limit plasma frequency shows a weak dependence on the spin polarization. We observe that when wave vector increases slightly, plasmon frequency in spin-polarized BLG is smaller than that in unpolarized case. However, at larger wave-vectors, the spin-polarization  $P$  increases significantly plasmon frequency compared to the case  $P=0$ . The plasmon curve of spin-polarized BLG merges the SPE boundary similarly as in unpolarized system [20]. Fig. 2(b) shows that the plasmons became damped at much smaller  $q$  due to spin-polarization and plasmon damping rate of unpolarized system shows no kink as already known because the SPE continuum of spin-up carriers is identical to that of spin-down ones.



**Fig. 2.** Plasmon frequency (a) and damping rate (b) in spin-polarized BLG ( $P=0.5$ ) and unpolarized BLG ( $P=0$ ) for  $n=10^{12} \text{ cm}^{-2}$ . Dashed-dotted lines show the boundaries of the SPE continuum.

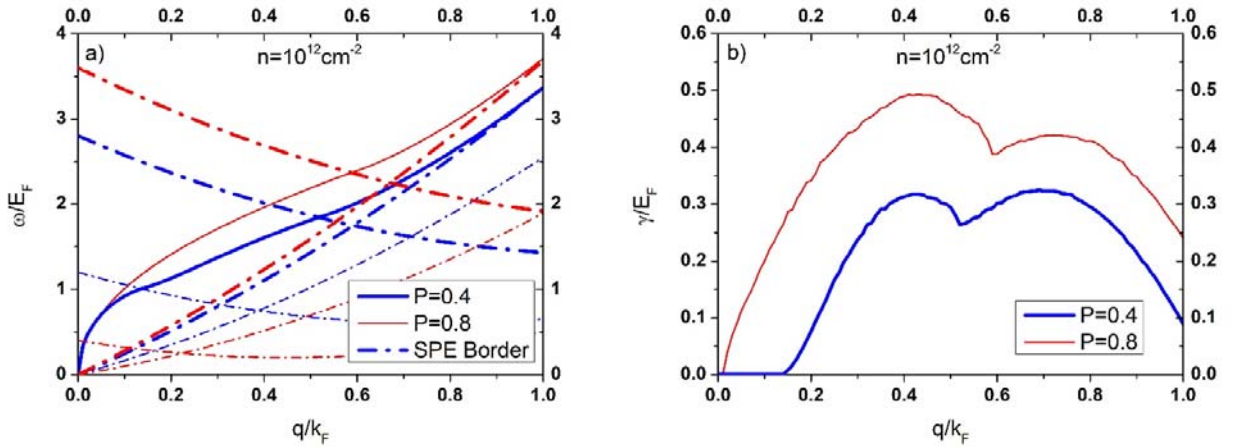


**Fig. 3.** Plasmon frequency (a) and damping rate (b) for spin-polarized BLG with  $n=10^{12} \text{ cm}^{-2}$  for  $P=0.4$  and  $P=0.8$ . Dashed-dotted lines show the boundaries of the SPE continuum.

In Fig. 3 we compare the plasmon frequency (left) and the damping rate (right) of plasma oscillations in partially polarized BLG with carrier density  $n=10^{12} \text{ cm}^{-2}$  in two cases  $P=0.4$  and  $P=0.8$ . As seen from the figure, for not too small wave-vector  $q$ , an increase in spin-polarization leads to a remarkable increase in plasmon frequency. In addition, Fig. 3(b) indicates that the energy loss in case  $P=0.8$  occurs at much smaller wave-vector, about  $q \approx 0.01k_F$ , compared to  $q=0.15k_F$  in case  $P=0.4$  and the damping rate in the former case is larger and has a local

minimum at larger  $q$  in comparison with the latter case. It is easily understood because as  $P$  increases the number of minority (majority) carriers decreases (increases), the lower edge of the inter-band continuum of minority (majority) spin carriers moves down (up) and the number of unoccupied states of minority carriers is larger, leading to stronger inter-band transitions.

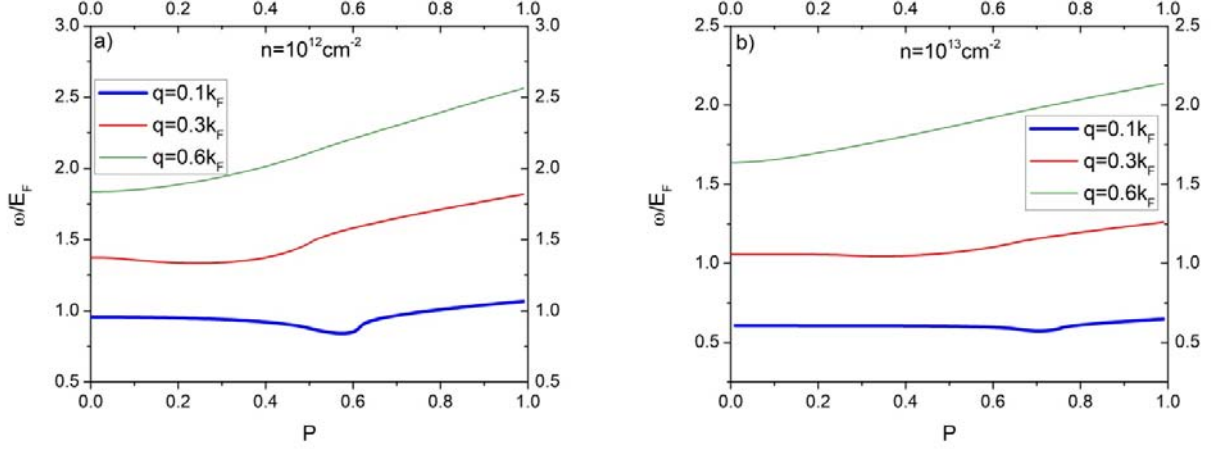


**Fig. 4.** Plasmon frequency as a functions of polarization  $P$  in spin-polarized BLG with  $n = 10^{12} \text{ cm}^{-2}$  (a) and  $n = 10^{13} \text{ cm}^{-2}$  (b) for several wave-vectors.

For more information about the effects of spin polarization on plasmon modes, we plot in Fig. 4 the plasmon frequency as a function of spin polarization in two cases  $n = 10^{12} \text{ cm}^{-2}$  and  $n = 10^{13} \text{ cm}^{-2}$  for several values of wave-vector. It is seen from the figures that the degree of spin polarization  $P$  affects slightly (strongly) plasmon frequency at small (large) wave-vectors.

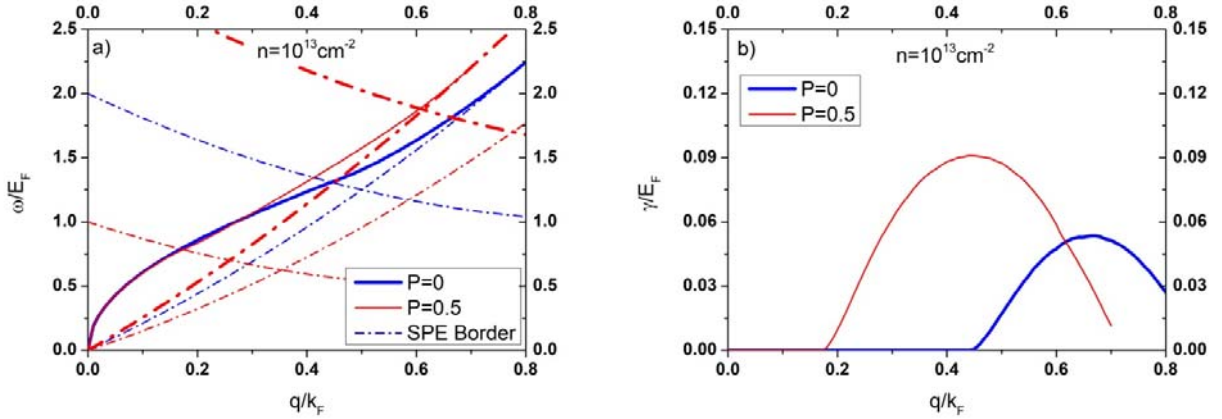


**Fig. 5.** Plasmon frequency (a) and damping rate (b) in spin-polarized BLG with  $n = 10^{13} \text{ cm}^{-2}$  for  $P=0.5$  and  $P=0$ . Dashed-dotted lines show the boundaries of the SPE continuum.

We now consider the effects of carrier density on plasmon characters in BLG. Fig. 5 demonstrates plasmon frequency (a) and the damping rate (b) in spin-polarized and unpolarized BLG with  $n = 10^{13} \text{ cm}^{-2}$ . Figs. 2(a) and 5(a) indicate that in both two cases  $P = 0$  and  $P = 0.5$  the increase in electron density decreases pronouncedly plasmon frequency. We also find from Fig. 5 that at large carrier densities the plasmon dispersion curve merges the upper edge of the intra-band continuum of majority spin carriers and vanishes before entering the inter-band continuum. Hence for  $n = 10^{13} \text{ cm}^{-2}$  the damping rate shows no kink as a function of  $q$  as in the case  $n = 10^{12} \text{ cm}^{-2}$ .

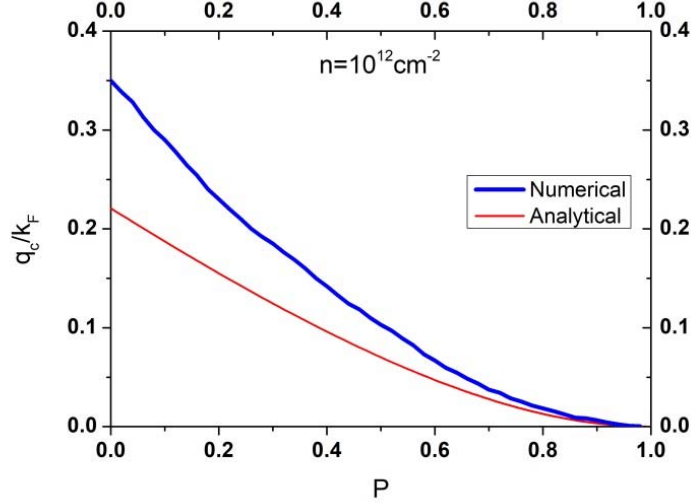


**Fig. 6.** The critical wave-vector  $q_c$  at which the plasmon dispersion curve hits the edge of the SPE of minority spin carriers.

Finally in Fig. 6 we show the analytical and numerical critical wave-vector  $q_c$  as a function of degree of spin polarization. The critical wave-vector decreases with increasing spin polarization because the lower edge of the interband continuum of the minority spin carriers moves down as  $P$  increases. For smaller  $P$  the lower edge of the interband continuum of minority spin carriers is higher and  $q_c$  is larger. Hence the long wavelength limit result for  $q_c$  is less correct and differs remarkably from the numerically calculated critical wave-vector. Note that our numerical value of  $q_c$  can be used to estimate the degree of spin polarization experimentally [32].

#### 4. Conclusion

In summary, the plasmon frequency and damping rate of plasma oscillations in a spin-polarized BLG system at zero-temperature have been calculated for the first time. Obtained analytical and numerical results indicate that plasmon frequency is dispersing as  $\sqrt{q}$  and almost independent of spin polarization in long wavelength limit. The plasmon frequency and damping rate decreases significantly with increasing substrate dielectric constant. We also find that the degree of spin polarization affects slightly (strongly) plasmon frequency at small (large) wave-vectors. The maximum value of damping rate increases with increasing  $P$  due to larger number of unoccupied states of minority carriers, leading to easier inter-subband e-h excitations. For large carrier density ( $n \sim 10^{13} \text{ cm}^{-2}$ ) the damping rate of partially polarized system shows no kink as a function of  $q$  similarly as in unpolarized case. However, in low density systems ( $n \sim 10^{12} \text{ cm}^{-2}$ ),  $\gamma$  of partially polarized BLG shows a local minimum when the plasmon curve hits the lower edge of the interband continuum of majority spin carriers. We have also calculated analytically and numerically the critical wave-vector  $q_c$  which can be used to determined the degree of spin polarization experimentally.

#### Acknowledgement

This research is funded by Vietnam National Foundation for Science and Technology Development (NAFOSTED) under grant number 103.01-2020.11.

#### References

- [1] Geim A K and Novoselov K S 2007 *Nature Mater* **6** 183.
- [2] Geim A K and MacDonald A H 2007 *Phys. Today* **60** 35.
- [3] Wei J, Zang Z, Zhang Y, Wang M, Du J and Tang X 2017 *Optics Letters* **42** 911.
- [4] Garcia de Abajo F J 2014 *ACS Photonics* **1** 135.
- [5] Koppens Frank H L, Chang D E and Garcia de Abajo F J 2011 *Nano Lett.* **11** 3370.

- [6] Avouris P and Freitag M 2014 *IEEE* **20** 6000112.
- [7] Ryzhii V, Ryzhii M, Mitin V, Shur M S, Satou A and Otsuji T 2013 *J. Appl. Phys.* **113** 174506.
- [8] Politano A, Pietro A, Di Profio G, Sanna V, Cupolillo A, Chakraborty S, Arafa H and Curcio E 2017 *Advanced Materials* **29(2)** 201603504.
- [9] Polini M, Asgari R, Borghi G, Barlas Y, Pereg-Barnea T and MacDonald A H 2008 *Phys. Rev. B* **77** 081411(R).
- [10] Politano A, Cupolillo A, Di Profio G, Arafat H A, Chiarello G and Curcio E 2016 *J. Phys. Condens. Matter* **28** 363003.
- [11] Ni G X, McLeod A S, Sun Z, Wang L, Xiong L, Post K W, Sunku S S, Jiang B -Y, Hone J, Dean C R, Fogler M M and Basov D N 2018 *Nature* **557** 530.
- [12] Lundeberg M B, Gao Y, Asgari R, Tan Ch, Duppen B V, Autore M, González P A, Woessner A, Watanabe K, Taniguchi T, Hillenbrand R, Hone J, Polini M and Koppens F H L 2017 *Science* **357** 187.
- [13] Sunku S S, Ni G X, Jiang B Y, Yoo H, Sternbach A, McLeod A S, Stauber T, Xiong L, Taniguchi T, Watanabe K, Kim P, Fogler M M and Basov D N 2018 *Science* **362** 1153.
- [14] Jiang B Y, Ni G X, Addison Z, Shi J K, Liu X, Zhao Sh Y F, Kim P, Mele E J, Basov D N and Fogler M M 2017 *Nano Lett.* **17** 7080.
- [15] Lundeberg M B, Lundeberg M B, Gao Y, Asgari R, Tan Ch, Duppen B V, Autore M, González P A, Woessner A, Watanabe K, Taniguchi T, Hillenbrand R, Hone J, Polini M and Koppens F H L 2017 *Nat. Mater.* **16** 204.
- [16] Ni G X, Wang L, Goldflam M D, Wagner M, Fei Z, McLeod A S, Liu M K, Keilmann F, Özyilmaz B, CastroNeto A H, Hone J, Fogler M M and Basov D N 2016 *Nat. Photon.* **10** 244.
- [17] Politano A, Yu H K, Farias D and Chiarello G 2018 *Phys. Rev. B* **97** 035414.
- [18] Koppens F H L, Mueller T, Avouris Ph, Ferrari A C, Vitiello M S and Polini M 2014 *Nat. Nanotechnol.* **9** 780.
- [19] Hwang E H and DasSarma S 2007 *Phys. Rev. B* **75** 205418.
- [20] Sensarma R, Hwang E H and DasSarma S 2010 *Phys. Rev. B* **82** 195428.
- [21] Hwang E H and DasSarma S 2007 2008 *Phys. Rev. Lett.* **101** 156802.
- [22] CastroNeto A H, Guinea F, Peres N M R, Novoselov K S and Geim A K 2009 *Rev. Mod. Phys.* **81** 109.
- [23] Maier S A 2007 *Plasmonics – Fundamentals and Applications* Springer, New York.
- [24] Wang X F and Chakraborty T 2010 *Phys. Rev. B* **81** 081402(R).
- [25] Khanh N Q and Linh D K 2018 *Superlatt. Microstruct.* **116** 181.
- [26] Linh D K and Khanh N Q 2018 *Superlatt. Microstruct.* **114** 406.
- [27] Khanh N Q 2011 *Physica E* **43** 1712.
- [28] Khanh N Q and Totsuji H 2004 *Phys. Rev. B* **69** 165110.
- [29] Davoudi B and Tosi M P 2002 *Physica B* **322** 124.
- [30] Perrot F and Dharma-wardana M W C 2001 *Phys. Rev. Lett.* **87** 206404.
- [31] Khanh N Q 2007 *Physica B* **396** 187.
- [32] Agarwal A and Vignale G 2015 *Phys. Rev. B* **91** 245407.
- [33] Vazifeshenas T, Amlaki T, Farmanbar M and Parhizgar F 2010 *Phys. Lett. A* **374** 4899.
- [34] Badalyan S M and Peeters F M 2012 *Phys. Rev. B* **85** 195444.
- [35] Zhu J -J, Badalyan S M and Peeters F M 2013 *Phys. Rev. B* **87** 085401.
- [36] Men N V, Khanh N Q and Phuong D T K 2019 *Sol. Stat. Commun.* **298** 113647.
- [37] Men N V, Khanh N Q and Phuong D T K 2019 *Sol. Stat. Commun.* **294** 43.
- [38] Men N V, Khanh N Q and Phuong D T K 2019 *Phys. Lett. A* **383** 1364.
- [39] Men N V, Khanh N Q and Phuong D T K 2020 *Physica E* **118** 113859.
- [40] Phuong D T K and Men N V 2020 *Phys. Lett. A* **384** 126221.
- [41] Tuan D V and Khanh N Q 2013 *Physica E* **54** 267.
- [42] Hwang E H and DasSarma S 2009 *Phys. Rev. B* **80** 205405.
- [43] Wunsch B, Stauber T, Sols F and Guinea F 2006 *New J. Phys.* **8** 318.
- [44] Svintsov D, Vyurkov V, Ryzhii V and Otsuji T 2013 *J. Appl. Phys.* **113** 053701.